ORIGINAL ARTICLE

Correlations between metabolic texture features, genetic heterogeneity, and mutation burden in patients with lung cancer

Seung Hwan Moon[1] · Jinho Kim[2] · Je-Gun Joung[2] · Hongui Cha[2,3] · Woong-Yang Park[4] · Jin Seok Ahn[5] · Myung-Ju Ahn[5] · Keunchil Park[5] · Joon Young Choi[1] · Kyung-Han Lee[1] · Byung-Tae Kim[1] · Se-Hoon Lee[3,5]

Abstract

Purpose This study investigated the correlations between parameters of ^{18}F-fluorodeoxyglucose (FDG) uptake on positron emission tomography (PET) scan and indices of genetic properties, heterogeneity index (HI), and tumor mutation burden (TMB), in patients with lung cancer.

Methods We produced 106 PET indices for each tumor site that underwent genomic analysis in a total of 176 study subjects (age, 62.0 ± 10.0 y; males, 68.2%), comprising 101 adenocarcinoma (ADC), 29 squamous cell carcinoma (SQCC), and 46 small cell lung cancer (SCLC) patients. We then examined the correlations of the PET parameters with genetic properties of HI and TMB, according to pathology and tumor site.

Results Comparisons between PET parameters and the genetic properties with false discovery rate (FDR) correction revealed that the surface standard uptake value (SUV) entropy of SUV statistics had a significant correlation with HI only in patients with SCLC who underwent a genetic test in lymph nodes ($r = 0.592$, $p = 0.028$), whereas PET parameters did not show a significant correlation with HI or TMB in patients with SCLC who underwent a genetic test in lung tissue. In patients with ADC and SQCC, there was no significant correlation between PET parameters and the genetic properties. Although SUV_{max} showed raw p values less than 0.05 in correlation with HI ($r = 0.315$, raw $p = 0.048$) and TMB ($r = 0.206$, raw $p = 0.043$) in ADC, and SUV_{peak} had a raw p value less than 0.05 in correlation with HI ($r = 0.394$, raw $p = 0.046$) in SQCC, these parameters were not significant when corrected by FDR.

Conclusions In this study, surface SUV entropy had a significant correlation with HI in SCLC. Regarding other PET parameters and tumors, no significant correlation with genetic parameters existed.

Keywords ^{18}F-fluorodeoxyglucose (FDG) · Positron emission tomography (PET) · Imaging genomics · Genetic heterogeneity · Tumor mutation burden

✉ Seung Hwan Moon
seunghwan.moons.moon@samsung.com

✉ Se-Hoon Lee
sehoon.lee@samsung.com

[1] Department of Nuclear Medicine and Molecular Imaging, Samsung Medical Center, Seoul, Republic of Korea

[2] Samsung Genome Institute, Samsung Medical Center, Seoul, Republic of Korea

[3] Department of Health Sciences and Technology, SAIHST, Sungkyunkwan University, Seoul, Republic of Korea

[4] Samsung Genome Institute, Samsung Medical Center, Samsung Advanced Institute of Health Science and Technology, Department of Molecular Cell Biology, Sungkyunkwan University School of Medicine, Seoul, Republic of Korea

[5] Division of Hematology/Oncology, Department of Medicine, Samsung Medical Center, Sungkyunkwan University School of Medicine, Seoul, Republic of Korea

Introduction

Imaging genomics, extraction of quantitative features from medical images and association of these data with genetic expression, has emerged as an important field in medical image research [1, 2]. By linking a large amount of image data to genomic data, image features may become a surrogate marker of genetic alterations and have great potential to advance the management of patients with cancer. This knowledge may improve the assessment of heterogeneity and identification of changes at the molecular level of tumors without invasive procedures. It may also improve decision making about where to perform a biopsy [3–5].

Indicators reflect the overall characteristics of the genome, as well as information on whether each gene has mutations or not, and can also be useful biomarkers for cancer treatment. Intra-tumor heterogeneity refers to genomic variations within a tumor, co-existence of primary tumor cells and genetically distinct subclonal populations, which occur through branched tumor evolution [6]. Heterogeneity probably has a significant role in the progression and metastasis of a tumor, which affects patient outcome and poses a significant challenge to personalized cancer medicine [7–9]. Tumor mutation burden (TMB), a measurement of the overall number of mutations carried by tumor cells, has been suggested as a potentially helpful marker for immunotherapy. A recent study suggested that a higher TMB predicts a favorable outcome to PD-1/PD-L1 blockade across diverse tumors [10]. The heterogenetic index (HI) and TMB are biomarkers that represent the overall characteristics of tumor genetics and may be useful for personalized cancer medicine. Finding a surrogate marker for these indices would be valuable, and image features may be an appropriate candidate, because they are alternative indicators that do not require biopsy for genetic analysis in different lesions.

Although there has been growing interest in imaging genomics in recent years, there are few studies based on ^{18}F-fluorodeoxyglucose (FDG) positron emission tomography/computed tomography (PET/CT). FDG PET/CT-derived features may be useful in revealing the genetic characteristics of cancer that fail to be revealed by CT or MRI because these indices reflect the metabolic status of the tumor, unlike the conventional image modalities. However, a few studies on FDG PET/CT have focused on the relationship between FDG uptake and genetic mutations in patients with lung cancer PET genomics [11–13]. The correlations between parameters obtained from FDG PET/CT and overall genetic characteristics, such as HI and TMB, have not been fully investigated. Whether or not PET/CT-derived indices, such as standard uptake value (SUV) statistics or texture features, can reflect genetic characteristics, such as heterogeneity of tumors or TMB, is not well known.

Therefore, in this study, we investigated the associations between genetic characteristics, heterogeneity, and mutation burden and FDG PET/CT features in patients with lung cancer.

Materials and methods

Subjects

The study candidates were 417 patients with histologically confirmed lung cancer who were enrolled in a database of the Samsung Genome Institute and who underwent ^{18}F-FDG PET/CT. All patients had undergone genomic analysis of their tumor tissue and had agreed that the data could be used in other studies. Among these, we excluded 82 patients who had no HI or TMB data. Of the remaining 335 patients, we excluded 132 with small tumor volume (less than 10 cm^3) from the analysis. In addition, we excluded 11 patients whose tumor tissue was obtained for genomic analysis after neoadjuvant therapy; nine patients with other than adenocarcinoma (ADC), squamous cell carcinoma (SQCC), or small cell lung cancer (SCLC); and seven patients whose tumor tissue was obtained at a site of distant metastases. Therefore, a total of 176 patients were finally included from this collected dataset and were divided into three groups of ADC, SQCC, and SCLC for study analysis. The process of subject selection is illustrated in Fig. 1. This study was approved by the Institutional Review Board, and the requirement for written informed consent was waived.

PET/CT imaging

All patients fasted for at least 6 h, and blood glucose was <200 mg/dl at the time of the FDG injection. PET/CT without intravenous or oral contrast was performed on a GE Healthcare (Milwaukee, WI, USA) Discovery LS ($n = 56$) or Discovery STe ($n = 120$) scanner. At 60 min after injecting 225–417 MBq FDG, transmission scans were acquired from the skull base to mid-thigh at 4 min per frame in 2-D mode (Discovery LS) or 2.5 min per frame in 3-D mode (Discovery STe). Whole-body spiral CT was performed with an 8-slice helical CT (140 KeV, 40 to 120 mAs adjusted to body weight; section width = 5 mm) for the Discovery LS scanner and a 16-slice helical CT (140 KeV, 30 to 170 mAs with AutomA mode; section width = 3.75 mm) for the STe scanner. Attenuation-corrected PET images (voxel size = $4.3 \times 4.3 \times 3.9$ mm for Discovery LS, $3.9 \times 3.9 \times 3.3$ mm for Discovery STe) were reconstructed using CT data and 2-D (28 subsets, two iterations; Discovery LS) or 3-D ordered-subset expectation maximization algorithms (20 subsets, two iterations; STe).
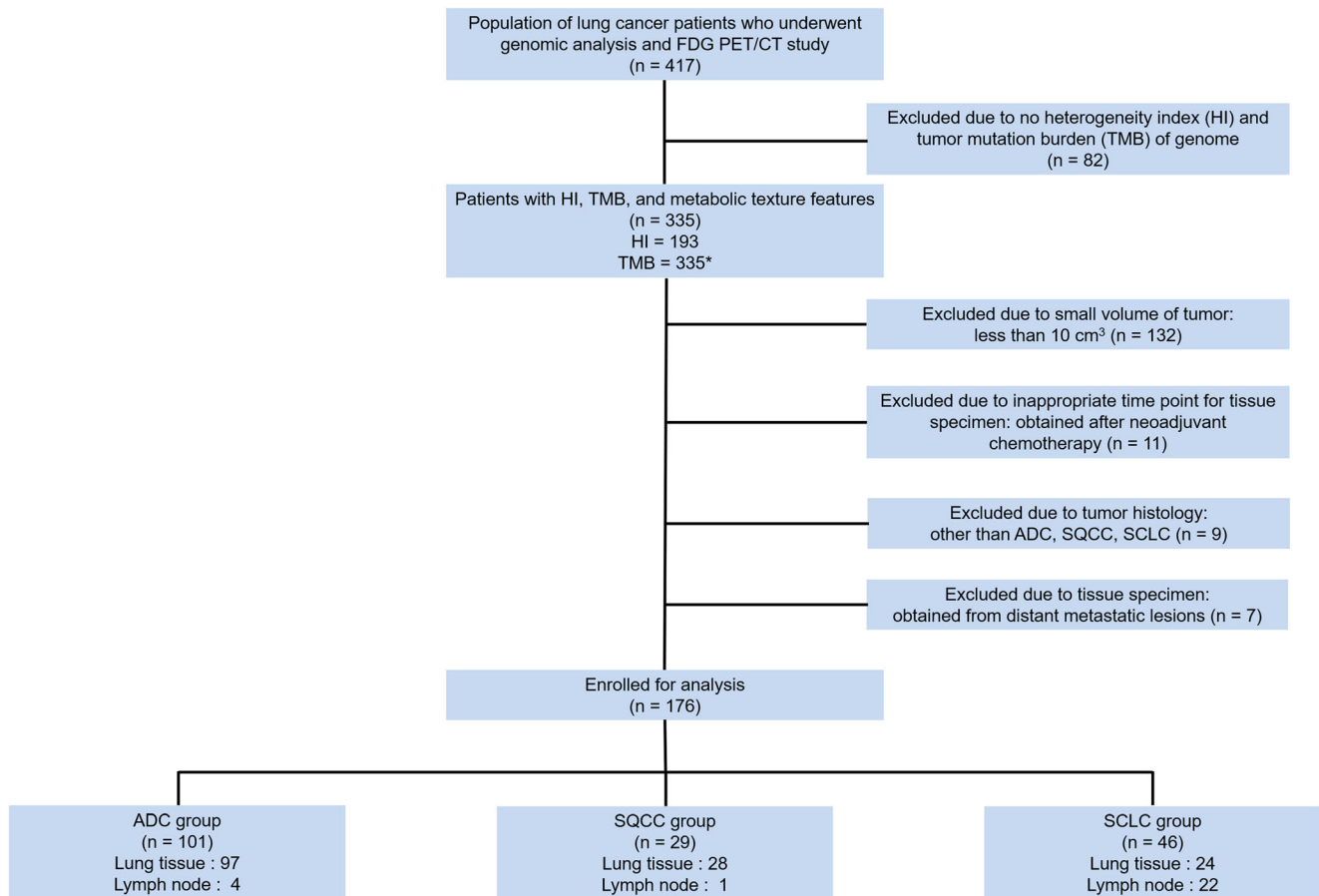
Fig. 1 Flow diagram of patient inclusion, with reason for exclusion and total study population

PET image analysis

To investigate the correlations between PET parameters and genomic characteristics, we performed image analysis on tumors in which tissue biopsy was performed for genomic analysis.

PET textural analysis was based on a previous study using the gradient-based segmentation method ('PET Edge') of MIM version 6.4 software (MIM Software Inc., Cleveland, OH, USA) [14]. The target tumor was identified by an experienced nuclear medicine physician (S.H.M) who was unaware of clinical information except the target tumor site. As the physician drags the cursor out from the center of the target tumor to a point near the edge of the lesion, six axes interactively extend out and the length of an axis is restricted when a large gradient is detected along that axis. Then, the software automatically outlines a three-dimensional volume of interest (VOI) on the tumor. After creating a gradient-based segmentation, we created an additional eight intensity-based segments by changing thresholds based on mediastinal blood pool (MBP) activity, liver activity, absolute SUV, and fixed percentage of maximum SUV (SUV_{max}).

For thresholds using MBP and liver activities, a VOI consisting of $5 \times 5 \times 1$ voxels was manually drawn at the aortic arch and right hepatic lobe at the level of the hepatic hilum, and the average SUV plus two standard deviations of each VOI was adopted as the threshold. Absolute SUV thresholds were fixed values of SUV 2.5, 3.0, 3.5, and percentage thresholds were 20%, 30%, and 40% of SUV_{max} on the tumor segmented by a gradient-based method. Therefore, nine different segmentations were automatically generated.

The textural analysis was performed using the Chang-Gung Image Texture Analysis toolbox (CGITA, http://code.google.com/p/cigita); this is an open-source software package implemented in MATLAB (version 2012a; MathWorks Inc., Natick, MA, USA) [15]. A total of 86 PET parameters available in CGITA were measured on the nine segments (Supplemental Table 1). Consequently, 774 PET parameters were generated per one measured target tumor lesion. The reason for obtaining the PET parameters through the nine different segmentation methods, consisting of one gradient-based method and an additional eight intensity-based methods, was to identify relatively robust indicators less affected by the image segmentation. Based on our experience, the additional intensity-based methods have been chosen from among commonly used methods. Details for selecting robust indicators are described in the "Statistical analysis". The metabolic tumor volume, obtained through the gradient-based

segmentation method, was used as a volume indicator to determine whether or not the measured target tumor was included in the subject enrollment process (Fig. 1).

Measurement of tumor heterogeneity and tumor mutation burden

Details of DNA extraction, library preparation, and sequencing were described in a previous study [16]. Genomic DNA was extracted using QIAamp DNA mini kits (Qiagen, Valencia, CA, USA), Promega Maxwell 16 CSC DNA FFPE kit, or a QIAamp DNA FFPE Tissue kit. Concentration, purity, and degradation of DNA were measured using a Nanodrop 8000 UV-Vis spectrometer (Thermo Scientific, Waltham, MA, USA), Qubit 2.0 Fluorometer (Life Technologies, Grand Island, NY, USA), and a 200 TapeStation Instrument (Agilent Technologies, Santa Clara, CA, USA), respectively. Target capture was performed using the SureSelect XT Reagent Kit, HSQ (Agilent Technologies), and a paired-end sequencing library was constructed with a barcode. Sequencing was performed on a HiSeq 2500 with 100-bp reads (Illumina, San Diego, CA, USA).

Heterogeneity measurement was based on Shannon's index, which is a popular index to measure species diversity [17]. For the set of variant allele frequency (VAF) of mutated loci in each tumor, VAFs I [0, 100] were obtained and assigned to one of bins (bin size = 10), and then Shannon's index was calculated with the distribution of probabilities of belonging to the bins.

TMB is the total number of non-synonymous mutations in a DNA coding region. We used the somatic nucleotide variant results of the CancerSCAN panel sequencing platform to calculate TMB [16]. To obtain only non-synonymous mutations, we performed filtering processes. First, non-coding alterations were excluded. Then germline variants were removed using public data such as ExAC and KRGDB. Lastly, truncation mutations were excluded since CancerSCAN includes genes that are already known to function in cancer. The number of filtered mutations was divided by the length of the target coding region to produce the TMB.

Statistical analysis

Statistical analysis was performed using SAS version 9.4 (SAS Institute, Cary, NC, USA) and R 3.0.2 (Vienna, Austria; http://www.R-project.org/).

Comparison of HI, TMB, and metabolic tumor volume according to histology was performed using the Kruskal-Wallis test. Rank transformation of these parameters was done, and Tukey's test was used over these ranks for post-hoc analysis.

The coefficient of variance (CV) in PET parameters from the nine segmentations of target tumor was calculated in enrolled subjects. The variables with a mean CV less than 0.1 were defined as robust variables that were less affected by the segmentation method. Among the 86 PET variables obtained using gradient-based segmentation, the robust variables were enrolled for further analysis to assess the correlations of PET parameters with HI and TMB. Pearson's correlation coefficient was used when both PET and genomic parameters were normally distributed; otherwise, Spearman's correlation coefficient was used.

When we conducted comparisons between PET and genomic variables, false discovery rate (FDR), a statistical approach for multiple comparisons, was used to correct random events that falsely appear significant.

A heat map was generated from PET texture metrics to reflect the different correlations with HI and TMB under several conditions.

All tests were two-sided, and p values less than 0.05 were considered statistically significant.

Results

Characteristics of subjects

The characteristics of the study patients are summarized in Table 1. They had a mean age (± standard deviation) of 62.0 ± 10 years (range 28 to 87 years), and the majority had ADC (57.4%). Among the total of 176 tumor lesions on which PET parameter measurements and genomic analysis were performed, all had TMB, and 113 had both TMB and HI (64.2%, 113/176). The remaining 63 lesions had only TMB without HI (35.8%, 63/176). The mean HI was 1.4 ± 0.3 (median 1.4; range 0.4 to 1.9), and mean TMB was 8.1 ± 4.9 (median 7.3; range 0.0 to 29.4).

Genetic parameters in ADC were lower than those of other lung cancers. The HI of the ADC group was significantly lower than that of the SQCC, SCLC (lung), and SCLC (lymph node) groups ($p = 0.016$, < 0.001, < 0.001, respectively). The TMB of the ADC group was also significantly lower than that of the SQCC group ($p = 0.012$). There was no significant difference between HI and TMB in the other groups. Tumor volume in this study was different according to pathology and biopsy site. The SCLC tumors obtained from the lung had a larger volume than ADC, SQCC, and SCLC tumors of the lymph node ($p < 0.001$, 0.010, < 0.001, respectively). Details of the HI, TMB, and metabolic tumor volume are presented in Table 2.

A total of 149 tumor lesions were from lung tissue (84.7%, 149/176), and 27 lesions were from lymph nodes (15.3%, 27/176). In the 149 lung tissue lesions, 101 were obtained by surgical resection (67.8%, 101/149) or percutaneous needle

Table 1 Characteristics of study patients ($n = 176$)

Characteristics		n (%)
Age, years (range)		62.0 ± 10 (28–87)
Male		120 (68.2%)
Smoking	Smoker	059 (33.5%)
	Ex-smoker	054 (30.7%)
	Never-smoker	059 (33.5%)
	N/A	004 (02.3%)
ECOG Performance status	0	019 (10.8%)
	1	118 (67.0%)
	2	007 (04.0%)
	N/A	032 (18.2%)
Pathology	ADC	101 (57.4%)
	SQCC	029 (16.5%)
	SCLC	046 (26.7%)
AJCC TNM staging 7th		
T	1	26 (14.8%)
	2	80 (45.5%)
	3	39 (22.2%)
	4	21 (11.9%)
	N/A	10 (05.6%)
N	0	59 (33.5%)
	1	24 (13.6%)
	2	47 (26.7%)
	3	39 (22.2%)
	N/A	07 (04.0%)
M	0	110 (62.5%)
	1a	010 (05.7%)
	1b	028 (15.9%)
	N/A	028 (15.9%)

ECOG, Eastern Cooperative Oncology Group; N/A, not applicable; ADC, adenocarcinoma; SQCC, squamous cell carcinoma; SCLC, small cell lung cancer; AJCC, American Joint Committee on Cancer; T, tumor; N, node; M, metastasis

biopsy (10.1%, 15/149), and the other 33 were obtained by bronchoscopy biopsy (22.1%, 33/149). All lymph node lesions were obtained by fine needle aspiration biopsy. In ADC and SQCC, most tumors were obtained from lung tissue, whereas in SCLC, half were obtained from lung tissue, and the other half were obtained from lymph nodes. Details of tumor tissue according to histology are given in Table 3.

Variance of PET parameters

The PET parameters of this study consisted of 55 texture features and 31 non-texture features (SUV and intensity histogram, 25; texture spectrum, two; geometry, four). Of the 55 texture features, 16 had a mean CV with a value less than 0.1, these included short run emphasis, short-zone emphasis, normalized contrast, normalized entropy, normalized homogeneity, normalized dissimilarity, normalized inverse, difference moment, correlation, mean convergence, second angular moment, contrast, entropy, intensity, inverse difference moment, code entropy, and small number emphasis (Supplemental Table 1). Of the 31 SUV statistics features, 11 showed a mean CV less than 0.1, these included SUV_{max}, SUV SD, SUV bias-corrected kurtosis, entropy, peak SUV normalized by lean body mass (SUL_{peak}), surface area, surface SUV entropy, surface SUV SD, SUV_{max} prod surface area, entropy prod surface area, and SUL_{peak} prod surface area. Consequently, a total of 27 parameters were selected as robust variables and enrolled for further analysis. Supplemental Figure 1 shows the CV of PET parameters according to size.

Correlation of PET parameters with HI and TMB

We assessed the correlation of PET parameters with HI and TMB according to pathology and biopsy site. Among SCLC, surface SUV entropy of SUV statistics showed a significant correlation with HI even after FDR correction in the lymph node group in which tissues for genetic analysis were taken from a lymph node (Table 2). Surface SUV entropy was obtained by calculating the entropy from the histogram which was created from the intensities of the contour pixels in the target tumor. Texture features of PET had no significant correlation with HI or TMB. Although entropy of SUV statistics and a small number emphasis of the neighboring gray level dependence (NGLD) matrix showed raw p values less than 0.05 in correlation with HI ($r = 0.471$, raw $p = 0.020$, $r = 0.438$, raw $p = 0.042$, respectively), they were not significant

Table 2 Comparison of genetic characteristics and metabolic tumor volume according to pathology

Variables	ADC	SQCC	SCLC		P – value*
			Lung	LN	
Heterogeneity index ($n = 113$)	1.18 ± 0.27 ($n = 40$)	1.36 ± 0.07 ($n = 27$)	1.53 ± 0.19 ($n = 24$)	1.53 ± 0.20 ($n = 22$)	< 0.001
Tumor mutation burden ($n = 176$)	7.35 ± 5.18 ($n = 101$)	9.87 ± 4.46 ($n = 29$)	8.68 ± 4.02 ($n = 24$)	9.02 ± 4.34 ($n = 22$)	0.007
Metabolic tumor volume ($n = 176$)	50.86 ± 75.19 ($n = 101$)	74.29 ± 90.00 ($n = 29$)	132.89 ± 95.04 ($n = 24$)	38.30 ± 29.35 ($n = 22$)	< 0.001

*Kruskal-Wallis test

Table 3 Correlation between genetic characteristics and metabolic texture features

Pathology	Matrix	Feature Names	Heterogeneity index						Tumor Mutation Burden					
			Correlation coefficient, raw p-value, FDR p value						Correlation coefficient, raw p value, FDR p value					
ADC			Lung ($n = 36$)			Lung + LN (n = 40)			Lung ($n = 97$)			Lung + LN (n = 101)		
	SUV statistics	SUV$_{max}$	0.330	0.049	0.883	0.315	0.048	0.891	0.206	0.043	0.871	0.188	0.060	0.873
SQCC			Lung ($n = 26$)			Lung + LN (n = 27)			Lung ($n = 28$)			Lung + LN (n = 29)		
	SUV statistics	SUL$_{peak}$	0.379	0.062	0.777	0.394	0.046	0.663	−0.029	0.886	0.954	0.044	0.824	0.989
SCLC			Lung (n = 24)			Lung (n = 24)			Lung (n = 24)			LN (n = 22)		
	SUV statistics	Entropy	−0.137	0.522	0.990	0.491	0.020	0.123	−0.021	0.921	0.997	−0.162	0.471	0.967
	SUV statistics	Surface SUV entropy	−0.012	0.956	0.990	0.592	0.004	0.028	0.001	0.997	0.997	−0.168	0.456	0.967
	NGLD	Small number emphasis	0.162	0.450	0.990	0.438	0.042	0.209	0.257	0.226	0.931	0.022	0.922	0.967

Consisted only of features showing significant correlation in raw p-value; ADC, adenocarcinoma; LN, lymph node; SQCC, squamous cell carcinoma; SCLC, small cell lung cancer; NGLD, neighboring gray level dependence

when they were corrected by the FDR method. In ADC and SQCC, there was no significant correlation between PET parameters, HI, and TMB (Table 3). SUV$_{max}$ had raw p values less than 0.05 in correlation with HI ($r = 0.315$, raw $p = 0.048$) and TMB ($r = 0.206$, raw $p = 0.043$) in patients with ADC, and SUV$_{peak}$ also had raw p values less than 0.05 in correlation with HI ($r = 0.394$, raw $p = 0.046$) in patients with SQCC. However, these parameters were not significant after FDR correction. Correlations of PET parameters and the genetic properties in different tumors are visualized in Supplemental Figure 2.

Discussion

There have been continued attempts to extract quantitative features from medical images and relate them to tumor genetics. Finding a link between these two pieces of information was expected to be a discovery that could advance precision medicine in patients with cancer [1, 2]. Extensive genetic heterogeneity caused by genomic instability exists between and within tumors and affects key cancer pathways, disease progression, and treatment response [7, 18]. Wide and extensive genetic testing of intra- and inter-genetic heterogeneity is required to identify the overall genetic variation of the tumor. Although biopsy is the gold standard for determining tumor genetics, it has the disadvantage that the diagnosis may be delayed due to the surgical planning and preparation process [19]. In addition, all tumors could not be sampled for genetic testing, and it is difficult to repeat the biopsy each time a recurrence is suspected. Even if a patient has a single tumor lesion, generally only a part of the tumor is used for the test. Consequently, it is difficult to identify genetic properties throughout the whole tumor in the clinic. Thus, it would assist decision making about when or where to perform a biopsy if it is possible to approximate the overall genetic characteristics of

the tumor. Image genomics has the potential to provide such information without the need to obtain tumor tissues from multiple sites.

The genetic properties of tumors, such as HI and TMB, can influence the course of treatment and clinical outcomes. Cancer cells can have considerable heterogeneity, which is likely to play a fundamental role in the phenotypic diversity observed in lung cancer, renal cell cancer, breast cancer, colorectal cancer, bladder cancer, prostate cancer, and glioma [7–9]. Previous research supports that intra-tumor heterogeneity has a significant prognostic value and impacts our understanding and management of cancer [6–9]. TMB has emerged as a sensitive marker in predicting response to immune checkpoint inhibitors and is more closely related to the response to PD-1 and PD-L1 blockade immunotherapy than PD-1 or PD-L1 expression measured by immunohistochemistry in patient with metastatic urothelial carcinoma [20]. Investigating the association of image features with HI and TMB is meaningful in finding a potential surrogate marker.

Computing textural features of FDG PET/CT might be useful in the quantification of heterogeneity [21] and may have an association with the genetic alteration of tumors. However, a few FDG PET/CT studies have reported the relationship between FDG uptake expressed in SUV statistics and genetic mutations in patients with lung cancer [12, 13]. Correlation between texture features of PET and tumor mutation in lung cancer has not yet been revealed. Above all, overall properties of tumor genes such as heterogeneity and mutation burden have not been investigated in terms of image genomics with FDG PET/CT.

In this study, associations of PET parameters with HI and TMB are different according to tumor pathology and site. In SCLC, surface SUV entropy, the entropy over the pixel intensities on the contour of target lesion, of the lymph group showed significant correlation with HI, whereas surface SUV entropy of the lung group did not. Moreover, the

directions of the correlation of these two groups were opposite (Table 3). We could not observe a difference in other cancers because the number of subjects in the lymph node group was too small. The discrepancy in the result with the same tumor pathology may be due to the different tissues where the tumor was involved. Cancer cells that invade lymph nodes may be a different subpopulation than cells that invade lung tissue, even though they are both identified as SCLC. Furthermore, technical issues are also likely to be involved in this result. In SCLC, the tumor volume and biopsy methods were significantly different between the lung group and lymph node group. The lymph node group had a smaller mean tumor volume than the lung group, and the tumor tissue was obtained for genetic testing by fine needle aspiration biopsy, unlike in the lung group. Tumor size affects the measurement of PET parameters [22–25], and the tumor volume and biopsy method may also affect the result of the genetic properties because the proportion of cancer cells for testing the whole tumor was determined by these factors.

The degree of FDG uptake, represented as SUV_{max} or SUV_{peak}, failed to show a significant correlation with HI or TMB in this study. FDG uptake in primary lung cancer is related with tumor cell proliferation, prognosis, and histopathological features of aggressiveness [26, 27]. It is generally accepted that tumors with a high FDG uptake have a higher likelihood of aggressiveness than those with a low FDG uptake [26]. As the genetic heterogeneity and mutation rate increase, the phenotypic features related to aggressiveness might become more prominent [6–9]. Based on this, we assumed that SUV, which is known to be associated with aggressiveness, might be related to HI and TMB. The results did not satisfy the initial assumption, which may be a sign that the hypothesis is not valid. However, this should be confirmed by further studies. SUV_{max} and SUV_{peak} showed raw p values less than 0.05 in correlation with the genetic properties, and the number of subjects enrolled in the study was not large. In particular, the small number of patients with HI did not have sufficient verification ability. In addition, the entropy of SUV statistics and the small number emphasis of the NGLD matrix in patients with SCLC also showed a raw p value less than 0.05 in correlation with HI. SUV_{max}, SUV_{peak}, the entropy of SUV statistics, and the small number emphasis of the NGLD are potential candidates to show significant associations with genetic properties in large-scale studies.

Several technical issues involving PET parameters are obstacles to generalizing the findings of this study and should be mentioned. First, metabolic tumor volume affects the measurement of PET parameters [22]. Heterogeneity of FDG uptake observed between diverse tumor volumes may not designate actual biologic differences between those tumors [23]. A previous study has shown that a minimum tumor volume of 45 cm³ is appropriate for texture analysis of FDG PET [23]. However, a larger scaled study with a greater number of

parameters suggested that the minimum metabolic tumor volume can be much smaller, approximately 10 cm³ [28]. In addition, certain PET parameters such as entropy and first-order statistical parameters are unaffected by tumor volume and provide reproducible values [24, 29]. In this study, tumors with more than 10 cm³ of metabolic volume were enrolled, and textural features of PET were obtained.

PET parameters are affected by the tumor segmentation method. Many algorithms based on either fixed or adaptively selected thresholds have been used to delineate target tumors in PET images. Advanced algorithms to perform semi-automated delineation are also proposed [30]. However, the difference of the measured values according to the used algorithm is not small, and the results of published validation studies are insufficient or inconsistent [30], which makes it difficult to use a certain algorithm as a standard. In this study, variance of the PET parameters, according to segmentation method, was evaluated and, among a total of 86 parameters, 27 that were unlikely to be affected by the segmentation method were selected for analysis. This inevitably limited the parameters to be evaluated, but probably minimized the errors caused by the segmentation method.

Textural features of PET also depend on the conditions of image acquisition. Even though there was a difference in degree, the features exhibited variations due to different acquisition modes and reconstruction parameters [21, 31, 32]. Therefore, unless the parameters are obtained under the same acquisition modes and reconstruction parameters, a study could not be considered to have a supreme quality. Unfortunately, texture features of this study were obtained from two different scanners (Discovery STe and Discovery LS). The proportion of SQCC was higher in the STe group than in the LS group (21.7 vs 5.4%, $p = 0.005$). Otherwise, there was no significant difference in the characteristics including age, gender, smoking history, performance, and staging between the two groups (Data not shown). The images acquisition with different scanners would inevitably have reduced the quality of this study.

Along with challenges including technical issues and need for standardization [5], the fundamental challenge of PET image genomics should be considered. In general, it is difficult to be certain that the results of the genome analysis fully reflect the genetic characteristics of the entire tumor, since only a small subset of the entire tumor is used for genetic testing. On the other hand, the indicators obtained from the image analysis reflect the characteristics of the whole tumor. Therefore, assessment of the correlation between PET parameters and genetic properties may be inappropriate if genetic analysis is not performed on multiple regions within the tumor. Image genomics in relation to multiregional genetic testing should be confirmed in further studies.

This study has several limitations. First, the relatively small and clinically heterogeneous subjects provide suboptimal

statistical power for robust analysis. Also, the heterogeneity of study subjects including the scanner, reconstruction method, tumor volume, and biopsy method may restrict generalization of the study results. Additional studies with large-scaled homogeneous subjects may thus be warranted to confirm the findings of this study.

In conclusion, significant correlation existed only in a small proportion of the total subjects in this study. Except the correlation between surface SUV entropy and genetic heterogeneity only in SCLC, no significant correlation was found in other PET parameters and tumors. However, challenges with metabolic genomics, including the reproducibility and reliability of the features, and limitations of the present study have hampered the ability to generalize the results. Further large-scale studies are needed to verify the findings of this study and to evaluate whether PET parameters have the potential as a surrogate marker for genetic heterogeneity and mutation burden of tumors.

Compliance with ethical standards

Conflict of interest The authors declare that they have no conflict of interest.

Ethical approval All procedures performed in studies involving human participants were in accordance with the ethical standards of the institutional and/or national research committee and with the 1964 Helsinki Declaration and its later amendments or comparable ethical standards.

Informed consent The institutional review board approved that the requirement for written informed consents were waived in this study.

References

1. Bai HX, Lee AM, Yang L, Zhang P, Davatzikos C, Maris JM, et al. Imaging genomics in cancer research: limitations and promises. Br J Radiol. 2016;89:20151030.
2. Jaffe CC. Imaging and genomics: is there a synergy? Radiology. 2012;264:329–31.
3. Mazurowski MA. Radiogenomics: what it is and why it is important. J Am Coll Radiol. 2015;12:862–6.
4. Andreassen CN, Schack LM, Laursen LV, Alsner J. Radiogenomics - current status, challenges and future directions. Cancer Lett. 2016;382:127–36.
5. Sala E, Mema E, Himoto Y, Veeraraghavan H, Brenton JD, Snyder A, et al. Unravelling tumour heterogeneity using next-generation imaging: radiomics, radiogenomics, and habitat imaging. Clin Radiol. 2017;72:3–10.
6. Gerlinger M, Rowan AJ, Horswell S, Math M, Larkin J, Endesfelder D, et al. Intratumor heterogeneity and branched evolution revealed by multiregion sequencing. N Engl J Med. 2012;366:883–92.
7. Burrell RA, McGranahan N, Bartek J, Swanton C. The causes and consequences of genetic heterogeneity in cancer evolution. Nature. 2013;501:338–45.
8. Morris LG, Riaz N, Desrichard A, Senbabaoglu Y, Hakimi AA, Makarov V, et al. Pan-cancer analysis of intratumor heterogeneity as a prognostic determinant of survival. Oncotarget. 2016;7:10051–63.
9. Liu J, Dang H, Wang XW. The significance of intertumor and intratumor heterogeneity in liver cancer. Exp Mol Med. 2018;50:e416.
10. Goodman AM, Kato S, Bazhenova L, Patel SP, Frampton GM, Miller V, et al. Tumor mutational burden as an independent predictor of response to immunotherapy in diverse cancers. Mol Cancer Ther. 2017;16:2598–608.
11. Nair VS, Gevaert O, Davidzon G, Napel S, Graves EE, Hoang CD, et al. Prognostic PET 18F-FDG uptake imaging features are associated with major oncogenomic alterations in patients with resected non-small cell lung cancer. Cancer Res. 2012;72:3725–34.
12. Nair VS, Gevaert O, Davidzon G, Plevritis SK, West R. NF-kappaB protein expression associates with (18)F-FDG PET tumor uptake in non-small cell lung cancer: a radiogenomics validation study to understand tumor metabolism. Lung Cancer. 2014;83:189–96.
13. Gevaert O, Xu J, Hoang CD, Leung AN, Xu Y, Quon A, et al. Non-small cell lung cancer: identifying prognostic imaging biomarkers by leveraging public gene expression microarray data–methods and preliminary results. Radiology. 2012;264:387–96.
14. Hyun SH, Kim HS, Choi SH, Choi DW, Lee JK, Lee KH, et al. Intratumoral heterogeneity of (18)F-FDG uptake predicts survival in patients with pancreatic ductal adenocarcinoma. Eur J Nucl Med Mol Imaging. 2016;43:1461–8.
15. Fang YH, Lin CY, Shih MJ, Wang HM, Ho TY, Liao CT, et al. Development and evaluation of an open-source software package "CGITA" for quantifying tumor heterogeneity with molecular images. Biomed Res Int. 2014;2014:248505.
16. Shin HT, Choi YL, Yun JW, Kim NKD, Kim SY, Jeon HJ, et al. Prevalence and detection of low-allele-fraction variants in clinical cancer samples. Nat Commun. 2017;8:1377.
17. Magurran A. Measuring biological diversity. Oxford: Blackwell; 2004.
18. Sottoriva A, Kang H, Ma Z, Graham TA, Salomon MP, Zhao J, et al. A big bang model of human colorectal tumor growth. Nat Genet. 2015;47:209–16.
19. Chow D, Chang P, Weinberg BD, Bota DA, Grinband J, Filippi CG. Imaging genetic heterogeneity in glioblastoma and other glial tumors: review of current methods and future directions. AJR Am J Roentgenol. 2018;210:30–8.
20. Rosenberg JE, Hoffman-Censits J, Powles T, van der Heijden MS, Balar AV, Necchi A, et al. Atezolizumab in patients with locally advanced and metastatic urothelial carcinoma who have progressed following treatment with platinum-based chemotherapy: a single-arm, multicentre, phase 2 trial. Lancet. 2016;387:1909–20.
21. Hatt M, Tixier F, Pierce L, Kinahan PE, Le Rest CC, Visvikis D. Characterization of PET/CT images using texture analysis: the past, the present... Any future? Eur J Nucl Med Mol Imaging. 2017;44:151–65.
22. Hatt M, Cheze-le Rest C, van Baardwijk A, Lambin P, Pradier O, Visvikis D. Impact of tumor size and tracer uptake heterogeneity in

(18)F-FDG PET and CT non-small cell lung cancer tumor delineation. J Nucl Med. 2011;52:1690–7.

23. Brooks FJ, Grigsby PW. The effect of small tumor volumes on studies of intratumoral heterogeneity of tracer uptake. J Nucl Med. 2014;55:37–42.

24. Forgacs A, Pall Jonsson H, Dahlbom M, Daver F, M DD, Opposits G, et al. A study on the basic criteria for selecting heterogeneity parameters of F18-FDG PET images. PLoS One. 2016;11: e0164113.

25. Bashir U, Siddique MM, McLean E, Goh V, Cook GJ. Imaging heterogeneity in lung cancer: techniques, applications, and challenges. AJR Am J Roentgenol. 2016;207:534–43.

26. Higashi K, Ueda Y, Ayabe K, Sakurai A, Seki H, Nambu Y, et al. FDG PET in the evaluation of the aggressiveness of pulmonary adenocarcinoma: correlation with histopathological features. Nucl Med Commun. 2000;21:707–14.

27. Deng SM, Zhang W, Zhang B, Chen YY, Li JH, Wu YW. Correlation between the uptake of 18F-Fluorodeoxyglucose (18F-FDG) and the expression of proliferation-associated antigen Ki-67 in Cancer patients: a meta-analysis. PLoS One. 2015;10:e0129028.

28. Hatt M, Majdoub M, Vallieres M, Tixier F, Le Rest CC, Groheux D, et al. 18F-FDG PET uptake characterization through texture analysis: investigating the complementary nature of heterogeneity and functional tumor volume in a multi-cancer site patient cohort. J Nucl Med. 2015;56:38–44.

29. Cook GJ, O'Brien ME, Siddique M, Chicklore S, Loi HY, Sharma B, et al. Non-small cell lung Cancer treated with Erlotinib: heterogeneity of (18)F-FDG uptake at PET-association with treatment response and prognosis. Radiology. 2015;276:883–93.

30. Hatt M, Lee JA, Schmidtlein CR, Naqa IE, Caldwell C, De Bernardi E, et al. Classification and evaluation strategies of auto-segmentation approaches for PET: report of AAPM task group no. 211. Med Phys. 2017;44:e1–e42.

31. Galavis PE, Hollensen C, Jallow N, Paliwal B, Jeraj R. Variability of textural features in FDG PET images due to different acquisition modes and reconstruction parameters. Acta Oncol. 2010;49:1012–6.

32. Desseroit MC, Tixier F, Weber WA, Siegel BA, Cheze Le Rest C, Visvikis D, et al. Reliability of PET/CT shape and heterogeneity features in functional and morphologic components of non-small cell lung Cancer tumors: a repeatability analysis in a prospective multicenter cohort. J Nucl Med. 2017;58:406–11.